Carbohydrate Polymers 184 (2018) 20–29

Contents lists available at ScienceDirect

Carbohydrate Polymers

journal homepage: www.elsevier.com/locate/carbpol

Synthesis of a poly(ester) dendritic β-cyclodextrin derivative by "click" chemistry: Combining the best of two worlds for complexation enhancement

Luis José López-Méndez[a], Israel González-Méndez[a], Rodrigo Aguayo-Ortiz[b], Laura Dominguez[b], Sofía L. Alcaraz-Estrada[c], Yareli Rojas-Aguirre[d,*], Patricia Guadarrama[a,**]

[a] Instituto de Investigaciones en Materiales, Universidad Nacional Autónoma de México, Mexico City, 04510, Mexico
[b] Facultad de Química, Departamento de Fisicoquímica, Universidad Nacional Autónoma de México, Mexico City, 04510, Mexico
[c] División de Medicina Genómica, Centro Médico Nacional "20 de Noviembre"–ISSSTE, Mexico City, 03100, Mexico
[d] Facultad de Química, Departamento de Farmacia, Universidad Nacional Autónoma de México, Mexico City, 04510, Mexico

ARTICLE INFO

Keywords:
Click chemistry
β-Cyclodextrin
Poly(ester) dendrons
Inclusion complex

ABSTRACT

In spite of the progress in the cyclodextrins chemistry, the synthesis of monodisperse derivatives with a defined degree of substitution is still a challenge. In this work we present a novel dendritic material produced by combining βCD and second generation poly(ester) dendrons. The selective attachment of dendrons in the seven positions of the βCD-primary face was performed through a CuAAC click reaction, which along with a very simple work-up, allowed obtaining the monodisperse material in very high yields. The product showed a great aqueous solubility and an in vitro non-toxic profile. The enhanced complexation potential of the product was evidenced through the formation of an inclusion complex with albendazole, which presented a $K_c = 29636.17\ M^{-1}$. In this system, albendazole was 45 times more water-soluble in comparison to the complex albendazole-native βCD. All these features make the dendritic material very attractive for further applications in the formulation and drug delivery fields.

1. Introduction

Cyclodextrins (CDs) have been extensively considered for a number of chemical processes, ranging from the entrapment of hydrophobic guests, to molecular nanoreactors (Crini, 2014; Zhao & Zhong, 2012). Due to their chemical versatility, CDs can be widely assorted with charged groups, hydrophobic or hydrophilic moieties to tailor their physicochemical properties and recognition abilities, thus improving their performance. If the cavity of the modified CDs remains available, complexes may be formed with a single molecule or with a building block, leading to sophisticated supramolecular architectures with tunable properties (Schmidt, Hetzer, Ritter, & Barner-Kowollik, 2014). Native CDs and CD-based materials have played a significant role in pharmaceutical sciences (Loftsson & Brewster, 2012), and in the drug and gene delivery field (Antoniuk & Amiel, 2016). In this regard, βCD has been the most studied CD due to the suitable size of its cavity, which allows complexation with a wide range of drugs. However, its low aqueous solubility and nephrotoxicity have restricted its use in pharmaceutics and drug delivery. A number of βCD derivatives have been synthesized to overcome those limitations. Derivatizations have been used to increase the inclusion capacity, improve interaction with specific guests, and provide self-assembly abilities for the construction of drug delivery platforms (Varan, Varan, Erdoğar, Hincal, & Bilensoy, 2017).

The modification of βCD generally comprises amination, esterification or etherification reactions on the primary or secondary hydroxyl groups. Predominant functional groups incorporated to the macrocyle include alkyl, hydroxyalkyl, carboxyalkyl, amino, glucosyl, and sulfoalkyl groups (García, Leonardi, & Lamas, 2016; Ma, Zhang, & Xu, 2016; Stepniak, Lainer, Chmurski, & Jurczak, 2017). The latter has given rise to Captisol®, a βCD water-soluble sulfobutyl ether derivative (SBE-βCD) with a range of six to seven sulfobutyl ether substituents per CD molecule. Captisol® has strong solubilizing capacity, leading to the optimization of several pharmaceutical formulations. To date, eight FDA-approved Captisol-enabled® medications are currently marketed by different pharmaceutical companies (Captisol, 2017).

In spite of the progress on the CD chemistry, most of its derivatives, including SBE-βCD, are obtained with a random average degree of substitution, which is controlled by the relative molar ratio of the reagents, leading to poor batch-to-batch reproducibility. In addition,

* Corresponding author. Present address: Instituto de Investigaciones en Materiales, Universidad Nacional Autónoma de México, Mexico City, 04510, Mexico.
** Corresponding author.
E-mail addresses: udgwid_l@hotmail.com (L.J. López-Méndez), israel_025@hotmail.com (I. González-Méndez), rodaguayo@comunidad.unam.mx (R. Aguayo-Ortiz), lauraok@gmail.com (L. Dominguez), sofializeth@gmail.com (S.L. Alcaraz-Estrada), yareli.rojas@iim.unam.mx (Y. Rojas-Aguirre), patriciagua@iim.unam.mx (P. Guadarrama).

https://doi.org/10.1016/j.carbpol.2017.12.049
Received 15 September 2017; Received in revised form 14 December 2017; Accepted 17 December 2017
Available online 20 December 2017
0144-8617/

complicated synthetic paths using non-ecofriendly reagents and complex purification processes make it difficult to obtain products which meet the quality standards for pharmaceutical or drug delivery applications. Therefore, efficient syntheses to obtain monodisperse derivatives with defined substitution patterns are needed.

In this context we propose the engineering of a novel dendritic shape derivative, βCD[G2]-OH, with a defined substitution pattern, by combining βCD and poly(ester) second generation dendrons through an optimum synthetic process.

We selected 2,2-bis(hydroxymethyl)propionic acid (bis-MPA, 99% w/w) based poly(ester) second generation dendrons because of their water solubility and scaffolding ability. Moreover, their architecture is hydrolytically degradable, they are non-toxic and have shown strong potential for drug delivery (Carlmark, Malmström, & Malkoch, 2013; Juanola-Feliu, Colomer-Farrarons, Miribel-Catal, Samitier, & Valls-Pasola, 2012).

Hence, we hypothesize that the selective attachment of the poly (ester) dendrons in the primary face of βCD will produce a dendritic-shape derivative combining the physicochemical and biological features of both components, namely high aqueous solubility, no toxicity, enhanced complexation ability and potential to be used as drug carrier.

We anticipate that the poly(ester) dendrons could provide a suitable hydrophobic/hydrophilic balance since the polar bonds (C—O and C—N) and terminal hydroxyl groups would exceed the non-polar C—H groups on each dendritic branch, resulting in a very soluble product. Additionally, we expect that a particular H-bonding pattern at the periphery of the material will not distort the βCD cavity, preserving its availability to form inclusion complexes (ICs).

The synthesis of βCD[G2]-OH was addressed by initial preparing the poly(ester) dendrons with alkyne focal point and terminal —OH groups. These were then incorporated into the βCD primary face via the copper (I)-catalyzed azide-alkyne cycloaddition (CuAAC) in a selective manner. The influence of the dendrons on the βCD cavity accessibility was explored through a conformational analysis. The βCD[G2]-OH complexation potential, and its ability to enhance the solubility of hydrophobic molecules was evaluated using albendazole (ABZ) as a guest model. Finally, the cytotoxicity of the novel material was evaluated through assays in HeLa cells.

2. Materials and methods

2.1. Materials

Bis-MPA, 99% w/w, *p*-toluenesulfonic acid monohydrate (99% w/w), propargyl alcohol (99% w/w), sodium azide (NaN_3, 99% w/w), benzyl bromide (99% w/w), 2,2-dimethoxypropane (98% w/w), copper sulfate ($CuSO_4.5H_2O$, 99.99% w/w), 4-(dimethylamino) pyridine (DMAP, 99% w/w), iodine (99% w/w), DOWEX 50W-X2 resin, triphenylphosphine (PPh3, ≥98% w/w), Pd/C, *N,N´*-dicyclohexylcarbodiimide (DCC, 98% w/w), Sephadex LH-20, methanol (99.8%), dimethyl sulfoxide (DMSO) and L-ascorbic acid (99% w/w), were purchased from Sigma-Aldrich and used as received. βCD (98%, Sigma-Aldrich) was dried under vacuum before use while *N,N´*-dimethylformamide (DMF, Sigma-Aldrich) and methylene chloride (CH_2Cl_2, Sigma-Aldrich) were dried over CaH_2 before use.

HeLa cells were provided from Dr. Rosa Maria del Angel (20 de Noviembre-National Medical Center-ISSSTE); Gibco DMEM Advanced growth medium was purchased from Fisher Scientific and MTS cell proliferation assay kit was acquired from Promega™.

2.2. Synthesis

2.2.1. Synthesis of [G2]-$CO_2CH_2C_6H_6$ (1)

The synthesis of (1) was carried out as reported previously (Ihre, Hult, Fréchet, & Gitsov, 1998) with minor modifications. Briefly, bis-MPA (3.26 g, 18.70 mmol), benzyl-2,2-bis(methylol)propionate (2.00 g, 8.92 mmol), DPTS (0.806 g, 2.73 mmol) and DMAP (0.343 g, 2.8 mmol) were dissolved in CH_2Cl_2 (30 mL) under N_2 atmosphere. Then, DCC (4.60 g, 22.30 mmol) in CH_2Cl_2 was added and the mixture was stirred at RT for 24 h. The crude product was purified by column chromatography on silica gel, eluting with a mixture of EtOAc/hexane (8:2), and gradually modified to EtOAc/hexane 4:6, to obtain the product (4 g, 84% yield). EI+: *m/z* 536 [M]+; 521 [M-15 CH3]+;. ^{1}H NMR (400 MHz, $CDCl_3$; *δ*, ppm): 7.35 (s, 5H) —ArH, 5.17 (s, 2H) CH_2—Ar, 4.36 (s, 4H) —CH_2C, 4.12 (d, *J* = 11.9 Hz, 4H) —CH_2O, 3.59 (d, *J* = 11.9 Hz, 4H) —CH_2O, 1.42 (s, 6H) —CH_3, 1.35 (s, 6H) —CH_3, 1.32 (s, 3H) —CH_3, 1.10 (s, 6H) —CH_3. ^{13}C NMR (101 MHz, $CDCl_3$; *δ*, ppm): 173.46, 172.35, 135.46, 128.58, 128.37, 128.19, 98.02, 66.89, 65.88, 65.27, 46.79, 41.98, 25.06, 22.13, 18.41, 17.70. FT-IR (ATR, cm^{-1}): 2992, 2937, 2877, 1079, 831, 733.

2.2.2. Synthesis of [G2]-$CO_2CH_2C_6H_6$ (2)

This compound was synthesized following the protocol previously reported (Ihre, Padilla De Jesús, Szoka Francis, & Fréchet, 2002) (2.99 g, 99%). EI+: *m/z* 446 [M]+; 431[M-15]+; ^{1}H NMR (400 MHz, $CDCl_3$; *δ*, ppm): 4.32 (s, 4H) —CH_2C, 4.15 (d, *J* = 12.1Hz, 4H) —CH_2O, 3.62 (d, *J* = 12.1Hz, 4H) —CH_2O, 1.40 (s, 3H) —CH_3, 1.34 (s, 3H) —CH_3, 1.30 (s, 3H) —CH_3, 1.13 (s, 6H) —CH_3. ^{13}C RMN (101 MHz, $CDCl_3$; *δ*, ppm): 177.12, 173.60, 98.14, 65.93, 65.56, 41.95, 33.27, 24.49, 22.72, 18.57, 17.92. FT-IR (ATR, cm^{-1}): 3523, 2987, 2923, 2863, 1077, 829, 723.

2.2.3. Synthesis of [G2]-$CO_2CH_2C_2H$ (3)

Compound (2) (1.5 g, 3.4 mmol), propargyl alcohol (0.3 mL, 5.0 mmol), DMAP (20.7 mg, 0.17 mmol) and DPTS (182.4 mg, 0.62 mmol) were dissolved in CH_2Cl_2 (20 mL) and DCC (841.7 mg, 4.0 mmol) was added. The reaction proceeded at RT for 24 h. The DCU was removed, the filtrate was washed with CH_2Cl_2, and the crude product was purified by column chromatography under the conditions described for Section 2.2.1. (4.0 g, 86%). EI+: *m/z* [M]+; 484.5. ^{1}H NMR (400 MHz, DMSO-d_6; *δ*, ppm): 4.74 (d, *J* = 2.4 Hz, 2H) —CH_2C≡C, 4.23 (s, 4H) —CH_2C, 4.00 (d, *J* = 11.7 Hz, 4H) —CH_2O, 3.61 (d, *J* = 11.7 Hz, 4H) —CH_2O, 3.57 (t, *J* = 2.4 Hz, 1H) —C≡ C—H, 1.35 (s, 6H) —CH_3, 1.23 (s, 12H) —CH_3, 1.03 (s, 6H) —CH_3. ^{13}C NMR (101 MHz, DMSO-d_6; *δ*, ppm): 173.07, 171.49, 97.35, 77.91, 64.99, 64.82, 52.46, 46.30, 41.48, 25.56, 21.52, 17.87, 16.99. FT-IR (ATR, cm^{-1}): 3283, 2924, 2361, 1732, 1074, 833, 728, 516.

2.2.4. Synthesis of heptakis(6-deoxy-6-iodo)-β-cyclodextrin (β-CD-$(I)_7$) (4)

The synthesis of (4) was performed as earlier reported (Ashton, Königer, Stoddart, Alker, & Harding, 1996). The product, β-CD-$(I)_7$ (1.4 g, 85% yield) was dried under vacuum and characterized. MALDI-TOF: *m/z* 1926.96 [M+Na]+; m.p. > 200 °C; ^{1}H NMR (400 MHz, DMSO-d_6; *δ*, ppm): 6.01 (d, *J* = 5.48 Hz, 7H) OH-2, 5.90 (s, 7H) OH-3, 4.96 (d, *J* = 2.74 Hz, 7H) H-1, 3.78 (m, 7H) H-3, 3.61 (m, 14H) H-6a,b, 3.42 (m, 7H) H-5, 3.38 (m, 7H) H-4, 3.26 (m, 7H) H-2; ^{13}C NMR (101 MHz, DMSO-d_6; *δ*, ppm): 102.06, 85.88, 72.11, 71.85, 70.85, 9.38; FT-IR (ATR, cm^{-1}): 3327 (str. O—H), 1627 (str. C—O—H), 1412, 1331, 1149, 1035 (str. C—H).

2.2.5. Synthesis of heptakis(6-deoxy-6-azido)-β-cyclodextrin (β -CD-$(N_3)_7$) (5)

Compound (4) (0.6 g, 0.3 mmol) was dissolved in DMF (10 mL) at RT and NaN_3 (0.205 g, 3.86 mmol) was added. The mixture was reacted at 80 °C under N_2 atmosphere for 24 h. The DMF was vacuum removed; the solid was washed with water, lyophilized and β-CD-$(N_3)_7$ (0.38 g, 94% yield) was obtained. MALDI-TOF: *m/z* 1332 [M+Na]+; ^{1}H NMR (400 MHz, DMSO-d_6; *δ*, ppm): 5.88 (s, 7H) OH-2, 5.74 (s, 7H) OH-3, 4.88 (d, *J* = 2 Hz, 7H) H-1, 3.74 (m, 14H) H-6a,b, 3.59 (m, 7H) H-3, 3.55 (m, 7H) H-5, 3.38 (m, 14H) H-2, H-4; ^{13}C NMR (101 MHz, DMSO-d_6; *δ*, ppm): 101.98, 83.12, 72.51, 71.94, 70.25, 51.26. FT-IR (ATR,

cm^{-1}): 3331 (str. O—H), 2099 (str. N3), 1650 (str. C—O—H), 1438, 1285, 1152, 1041 (str. C—H).

2.2.6. Click reaction to obtain (6)

Compound (5) (0.05 g, 0.038 mmol) and compound (3) (0.142 g, 0.293 mmol) were dissolved in DMSO/water (5:1). $CuSO_4{\cdot}5H_2O$ (0.00826 g, 0.033 mmol, 0.8 eq.) was added and the addition of ascorbic acid was followed. The mixture was stirred at 50 °C for 24 h and concentrated under vacuum. The supernatant was re-suspended in methanol, filtered through zeolite and purified by size-exclusion chromatography (SEC) on a sephadex LH-20 column, using methanol as eluent to obtain the compound (6) (0.161 g, 91%). MALDI-TOF: *m/z* 4725.89 [M + Na] +; ^{1}H NMR (400 MHz, DMSO-d_6; δ, ppm): 7.95 (s, 7H) triazole, 6.01 (s, 7H) OH-2, 5.90 (s, 7H) OH-3, 5.01 (d, 21H) overlap OH-1/-CH_2-triazole, 4.48-4.32(m, 14H) H-6a,b, 4.18 (s, 28H)-CH_2C, 3.95 (d, J = 11.2 Hz, 21H) −CH_2O, 3.68 (s, 7H) H-3, 3.57 (d, J = 11.2 Hz, 21H) −CH_2O, 3.41 (s, 14H) H-4, H-5, 3.25 (s, 7H) H-2, 1.33 (s, 42H) −CH_3, 1.20 (s, 42H) −CH_3, 1.14 (s, 21H) −CH_3, 0.98 (s, 42H) −CH_3; ^{13}C NMR (101 MHz, DMSO-d_6; δ, ppm): 173.94, 173.0, 141.21, 126.23, 101.68, 97.32, 64.96, 64.53, 63.61, 57.69, 50.16, 46.09, 41.38, 25.33, 21.67, 17.76, 17.0, 16.63. FT-IR (ATR, cm^{-1}): 3356 (str. O—H), 2924, 1727, 1047 (str. C—O—H), 824, 729 (str. C—H).

2.2.7. Deprotection method to obtain of βCD[G2]-OH

Compound (6) (0.224 g, 0.054 mmol) was dissolved in 35 mL of MeOH, and 0.085 g of Dowex® 50WX2 was added afterwards. The reaction was stirred at RT during 6 h. The mixture was filtered and the solvent was vacuum removed to obtain βCD[G2]-OH (0.124 g, 99%). MALDI-TOF: *m/z* 4172.74 [M + CH_3OH] +; ^{1}H NMR (400 MHz, DMSO-d_6; δ, ppm): 7.93 (s, 7H), 5.99 (d, J = 6.1 Hz, 6H), 5.89 (s, 7H), 5.06 (s, 7H), 4.96 (q, J = 13.3 Hz, 14H), 4.62 (t, J = 5.5 Hz, 30H), 4.52 (d, J = 11.7 Hz, 7H), 4.33 (d, J = 12.8 Hz, 7H), 4.09 (d, J = 11.5 Hz, 28H), 3.68 (t, J = 8.5 Hz, 8H), 3.46–3.38 (m, 57H), 3.26 (d, J = 9.4 Hz, 8H), 3.19 (s, 7H), 1.11 (s, 23H), 0.98 (s, 42H); ^{13}C NMR (101 MHz, DMSO-d_6; δ, ppm): 173.98, 172.08, 141.17, 126.49, 101.66, 82.40, 72.19, 71.72, 69.32, 64.42, 63.66, 57.62, 50.18, 49.41, 46.03, 17.06, 16.61. FT-IR (ATR, cm^{-1}): 3349 (str. O—H), 2923, 1732, 1225, 1144, 1050 (str. C—O—H).

2.3. Nuclear magnetic resonance spectroscopy (NMR)

All NMR spectra were acquired at 25 °C in a Bruker Avance spectrometer (400 MHz for ^{1}H and 100 MHz for ^{13}C) under the Fourier transform mode using $CDCl_3$ and DMSO-d_6.

2.4. Differential scanning calorimetry (DSC)

DSC analyses were recorded on a Universal V4.5A TA Instruments USA. 5 ± 0.05 mg of each sample was placed in aluminum crimped pans. The heating rate was 10 °C/min, from 20 °C to 300 °C under N_2 flow.

2.5. UV–visible spectral analysis (UV–vis)

Solutions of ABZ (concentration range of 1.88×10^{-2} mM to 11.30×10^{-2} mM), βCD[G2]-OH and βCD[G2]-OH/ABZ (both in a concentration range of 0.13–0.30 mM) were prepared in a DMSO-water mixture (1:1) and analyzed in a UV300 UNICAM spectrophotometer with a quartz cell of path length of 1 cm.

2.6. Fourier transformed infrared spectroscopy (FTIR)

The FTIR spectra were recorded on Thermo Scientific Nicolet 6700 (4000–400 cm^{-1}).

2.7. Mass spectrometry (MS)

Mass spectra were taken in a JEOL JMS AX505 HA for the electronic impact mode and in a JEOL JMS AX102A (FAB +) Bruker omni-flex for the MALDI-TOF analyses.

2.8. Solubility tests

0.40 mg of βCD[G2]-OH was placed in a test tube, and 1 mL of solvent (*n*-hexane, toluene, ethyl acetate, tetrahydrofuran, dichloromethane, acetone, ethanol, methanol, acetonitrile, DMF and DMSO) was added. The mixture was stirred for 5 min at 25 °C. The aqueous solubility of βCD[G2]-OH was assessed by adding increasing amounts of the compound (5–985 mg) to a volume of 1 mL of water.

2.9. Molecular simulations

The βCD[G2]-OH model was constructed in the visual interface of Gaussian 09 (Frisch et al., 2009), and its geometry optimization was done with the MMFF 94 force field. A 100 ns molecular dynamics (MD) simulation of the βCD[G2]-OH was performed with the GROMACS 5.1.2 package and the AMBER99SB-ILDN force field (Abraham et al., 2015; Lindorff-Larsen et al., 2010) using the explicit solvent model TIP3P (Jorgensen, Chandrasekhar, Madura, Impey, & Klein, 1983) and neutralized with NaCl molecules. The energy minimization was launched with 5000 steps of steepest-descent at 300 K and bond lengths were constrained using the SHAKE algorithm (Forester & Smith, 1998).

The Molecular Mechanics/Poisson-Boltzmann solvent accessible surface area (MM/PBSA) algorithm (Kumari, Kumar, & Lynn, 2014) was used to calculate the polar and non-polar energy contributions to the solvation free energy (SFE) from the last 50 ns of the MD simulation.

The plots were generated with the Gnuplot 5.0 software, and the 3D figures were constructed with PyMOL v0.9 (DeLano, 2002).

2.10. Cytotoxicity

HeLa cells (50,000) were seeded in DMEM Advanced growth medium in 96-well plates and incubated (5% CO atmosphere at 37 °C). The culture medium was removed and each well was rinsed with DMEM Advanced to discard non-adherent cells. Afterwards, 100 µl of fresh medium containing βCD[G2]-OH (10, 1, 0.1, 0.01, and 0.001 mg/mL) were added. The samples were incubated during 48 h (37 °C, 5% CO) and the cell viability was evaluated through the MTS cell proliferation assay according to the CellTiter 96® Assay Technical Bulletin (Promega, 2012). Fresh DMEM with untreated cells was used as a control. The experiments were performed in triplicate and repeated three times (n = 9). The cell viability was computed as a percent of untreated controls.

2.11. Formation of the βCD[G2]-OH/ABZ inclusion complex (IC)

To obtain the IC we established the following cosolvency method: 5 mL of an aqueous solution of βCD[G2]-OH (15 mM) were mixed, in equimolar proportion, with 1 mL of an ethanolic suspension of ABZ. The mixture was stirred at 37 °C for 5 days, filtered and lyophilized to obtain the IC. A physical mixture (PM) of βCD[G2]-OH and ABZ was prepared in a 1:1 M ratio by grinding the two solids in a mortar.

2.12. Phase solubility study

The phase-solubility study was carried out according to the Higuchi & Connors method (Higuchi & Connors, 1965) with some modifications. Briefly, excess amounts of ABZ were added to aqueous solutions of βCD [G2]-OH in a concentration range from 5 to 30 mM. The samples were stirred at 37 °C for 5 days, filtered and analyzed in a UV–vis spectrophotometer at 296 nm for ABZ quantification. The apparent

complexation constant, K_c, was determined from the slope of the diagram, using the following equation:

$$K_c = (\text{slope}/S_o - \text{slope}) \quad (1)$$

where S_0 is the equilibrium solubility of ABZ in the absence of the host. Experiments following the procedure described above were performed using [G2]-OH in same range of concentrations (5–30 mM). For comparison purposes, this study was also carried out with βCD. However, the concentration range of the host was 2.7–16 mM due to the limited aqueous solubility of the βCD.

The complexation efficiency was computed using the equation

$$CE = \text{slope}/1 - \text{slope} \quad (2)$$

and the solubility enhancement factor (F) was determined with

$$F = S_{max}/S_o \quad (3)$$

where S_{max} is the highest solubility of ABZ in the presence of βCD[G2]-OH or βCD.

3. Results and discussion

3.1. Synthesis

The Construction of the βCD dendritic derivative, βCD[G2]-OH, was successfully performed (Scheme).

A first stage involved the synthesis, by a convergent approach, of second generation poly(ester) dendrons containing alkyne focal points, with the Steglich esterification as a key step to obtain them. Optimized reaction yields up to 80% were observed for (1) and (3) after the addition of DMAP and DPTS into the catalytic system (See Supplementary data). On the other hand, compound (2) was obtained in quantitative yields by a Pd/C catalyzed hydrogenolysis, according to previous reports (Ihre et al., 1998).

Prior to the development of any CD-based structure, CD macrocycles must be chemically modified at their primary and/or secondary face. Thus, a second stage of the synthetic work consisted in incorporating the azide functionality at the primary face of βCD, as counterpart of the alkyne group of (3) for the CuAAC click reaction. The synthetic sequence of selective peryodation of the hydroxyl groups of the primary face to obtain compound (4) was followed by the nucleophilic substitution with sodium azide to get the heptafunctionalized azide-βCD (5) in high yields.

The click reaction (CuAAC), that results in the formation of aromatic triazole moieties (Kolb, Finn, & Sharpless, 2001), has impacted the CDs chemistry in great extent, allowing their successful functionalization in a selective manner (Faugeras et al., 2012). Therefore, this was our method of choice for obtaining our βCD dendritic derivative. Compounds (3) and (5) were clicked and compound (6), containing acetal terminal groups, was obtained as a non-water-soluble solid. The reaction conditions that we set (DMSO:H_2O 5:1) proved to be excellent for quickly and easily achieving product yields up to 90%. It is worthy to mention that purification of (6) was conducted by exclusion size chromatography (using SEPHADEX LH-20), a high-yielding and much less cumbersome process compared to dialysis, the most common procedure used for the purification of these kind of materials.

Compound (6) was characterized by ^{1}H, and ^{13}C NMR, FT-IR and MS MALDI-TOF. With respect to ^{1}H NMR, the main signal, corresponding to the triazole group, appears at 7.95 ppm, which clearly confirms the formation of the click product. Additionally, singulets in 1.33 and 1.20 ppm indicate the presence of the acetal protecting groups, attached to the periphery of the dendrons. A complete substitution of the βCD was verified by MS in which a molecular ion of 4687 *m/z* is observed (Fig. S13 and S15 respectively). In FT-IR spectroscopy, the vibration of carbonyl groups corresponding to the dendrons appears at 1728 cm^{-1}, and a broad band was displayed at 3350 cm^{-1}, consistent with the unsubstituted hydroxyl groups in the secondary face of βCD.

To get βCD[G2]-OH, our target compound, a methanolysis of the acetal terminal groups was implemented in the presence of the acid resin DOWEX®. We must underscore that, in addition to its role in the deprotection reaction, the resin also allowed the removal of Cu (II), which has been considered one of the major drawbacks of the CuAAC click reaction (Svenson, 2015). In such a way, we successfully overcame this limitation and the product was easily obtained in quantitative yields.

The FT-IR spectrum of βCD[G2]-OH displayed a vibration band at 3400 cm^{-1}, corresponding to the OH groups, which is broader and more intense compared to the FT-IR spectrum of (6) due to the contribution of both, the hydroxyl groups of the deprotected dendrons and those corresponding to the βCD itself. The band at 1740 cm^{-1}, attributable to the carbonyl vibration of the poly(ester) groups was also observed.

A complete substitution at the seven positions of the βCD primary face after the click reaction was confirmed in the MS-MALDI TOF spectrum (Fig. 1) that displayed a signal at 4145.18 *m/z* corresponding to the βCD[G2]-OH molecular ion. The purity and monodispersity of the product was remarkable and additionally resulted in the absence of "chemical noise" that one often sees from the interaction of impurities with the MALDI-TOF matrix.

The ^{1}H, ^{13}C and HSQC NMR characterization of βCD[G2]-OH was carried out in DMSO-d_6. In the ^{1}H spectrum (Fig. 2), the signal at 7.95 ppm, corresponding to the triazole group, is key evidence that the click reaction took place. Additionally, the signals at 0.99 and 1.12 ppm are attributable to the dendritic methyl groups of second and first generation respectively. The βCD core was identified by the singlet at 5.07 ppm corresponding to the anomeric H-1, and by the broad signal at 5.92 ppm from the hydroxyl groups of the secondary face. ^{1}H-^{13}C HSQC experiments supported the βCD[G2]-OH characterization (Supporting information). The resolution between H-6´and H-6´´ (from the methylene group adjacent to the βCD glucopyranose) indicated that the average conformations of the CD macrocycle are gauche-gauche and gauche-trans, when the O5-C5-C6-N dihedral angle is analyzed, which is in agreement to previous reports (Schneider, Hacket, Rüdiger, & Ikeda, 1998).

3.2. Solubility tests

Several interesting questions arise when two functional molecular units like βCD and dendritic moieties come together. One is related to the impact of the derivatization on the solubility of the final product. To evaluate this parameter, solubility tests were performed in a range of solvents (Table S1 Supplementary information). Both aprotic and protic polar solvents were able to solvate the βCD[G2]-OH compound, indicating its intermolecular interaction versatility. Notably, the solubility of βCD[G2]-OH in water was extraordinarily high (> 95 g/100 mL), compared with that of βCD itself (1.8 g/100 mL) and some of its water-soluble derivatives (HPβCD and SBEβCD with 65 and 70 g/100 mL respectively) (Challa, Ahuja, Ali, & Khar, 2005) (Supplementary information). Thus, our design achieves a convenient hydrophilic/hydrophobic balance which places our dendritic derivative in a favorable position for biomedical and pharmaceutical applications.

3.3. Molecular simulation

To study the conformational behavior of the simulated βCD[G2]-OH system we conducted a 100 ns MD simulation of the molecule, solvated with explicit water molecules. The radius of gyration (Rg) was calculated during the simulation, maintaining small values related to compact and globular conformations (data not shown). At the end of the simulation, the conical shape of the βCD remained non-distorted, in agreement with our hypothesis.

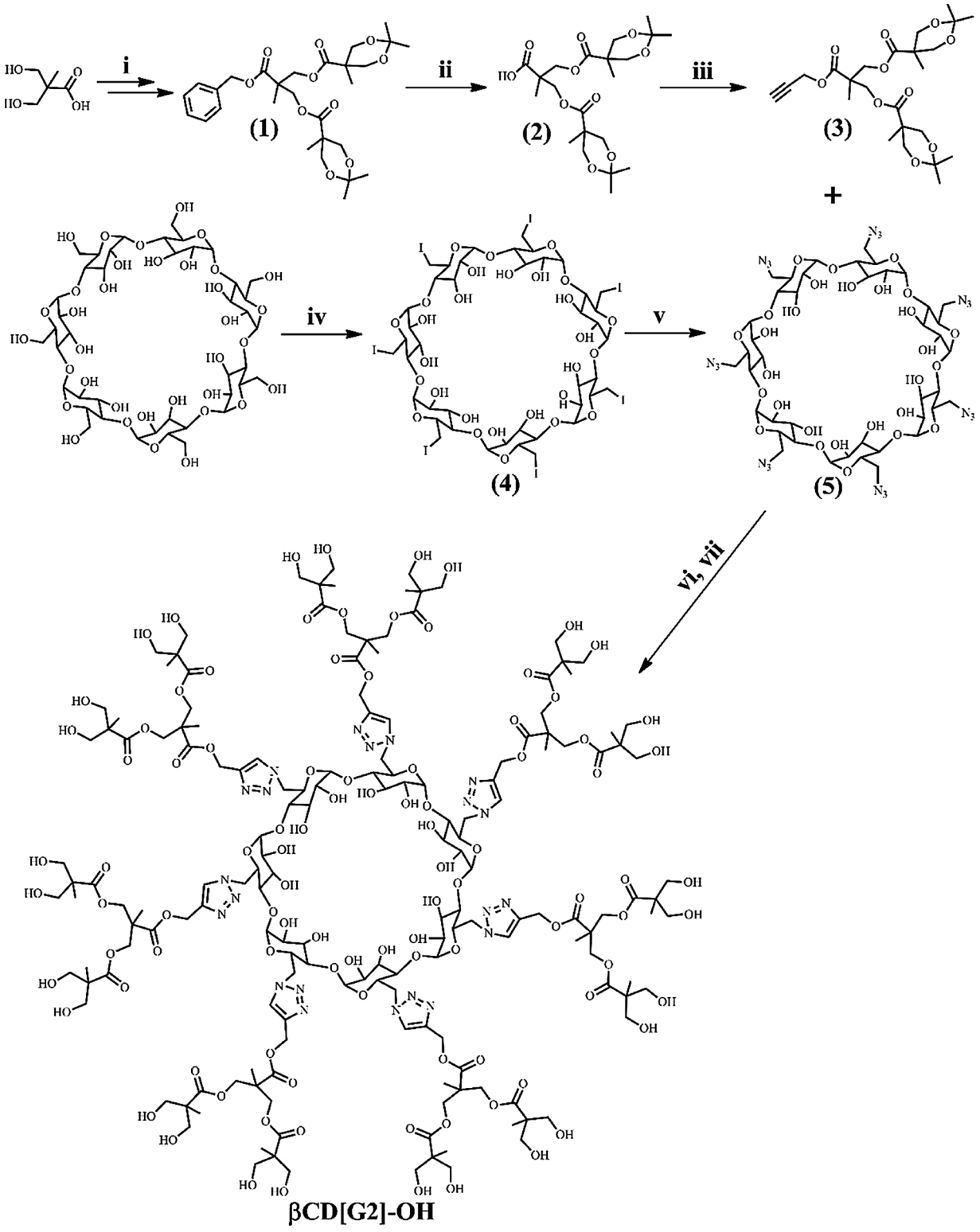

Scheme 1. Synthesis of βCD[G2]-OH: (i) DCC, DPTS, DMAP/CH_2Cl_2, RT, 24 h, (ii) H_2, Pd/C, AcOEt, (iii) propargyl alcohol, DCC, DPTS, DMAP, CH_2Cl_2, 23 °C, 24 h, (iv) I_2, Ph_3P/DMF, 70 °C, 18 h, (v) NaN_3, DMF, 80 °C, 24 h, (vi) Ascorbic acid, $CuSO_4.5H_2O$/DMSO:H2O (5:1), 50 °C, 24 h, (vii) Dowex® H^+/MeOH.

Under the MM/PBSA algorithm were estimated the electrostatic and nonpolar contributions to the SFE with a mean value of −203.7 ± 11 kJ/mol, corresponding to a favorable solvation of βCD [G2]-OH. This was experimentally observed in the solubility tests.

The diameter distribution was calculated, indicating that the substituted βCD exhibits a dynamic circular-/oval-shape during the simulation, being the circular one the most stable conformation through the last 10 ns of the MD simulation (Fig. 3A).

Since there is no apparent deformation of the βCD cavity due to the poly(ester) dendrons, we could infer that the dendronization does not hinder the complexation abilities of βCD[G2]-OH.

The dendrons effect on the βCD conformations was analyzed by the probability distribution of dihedral angles ω, (omega, O5-C5-C6-N6). Previous studies have reported that the most common ω angles in the

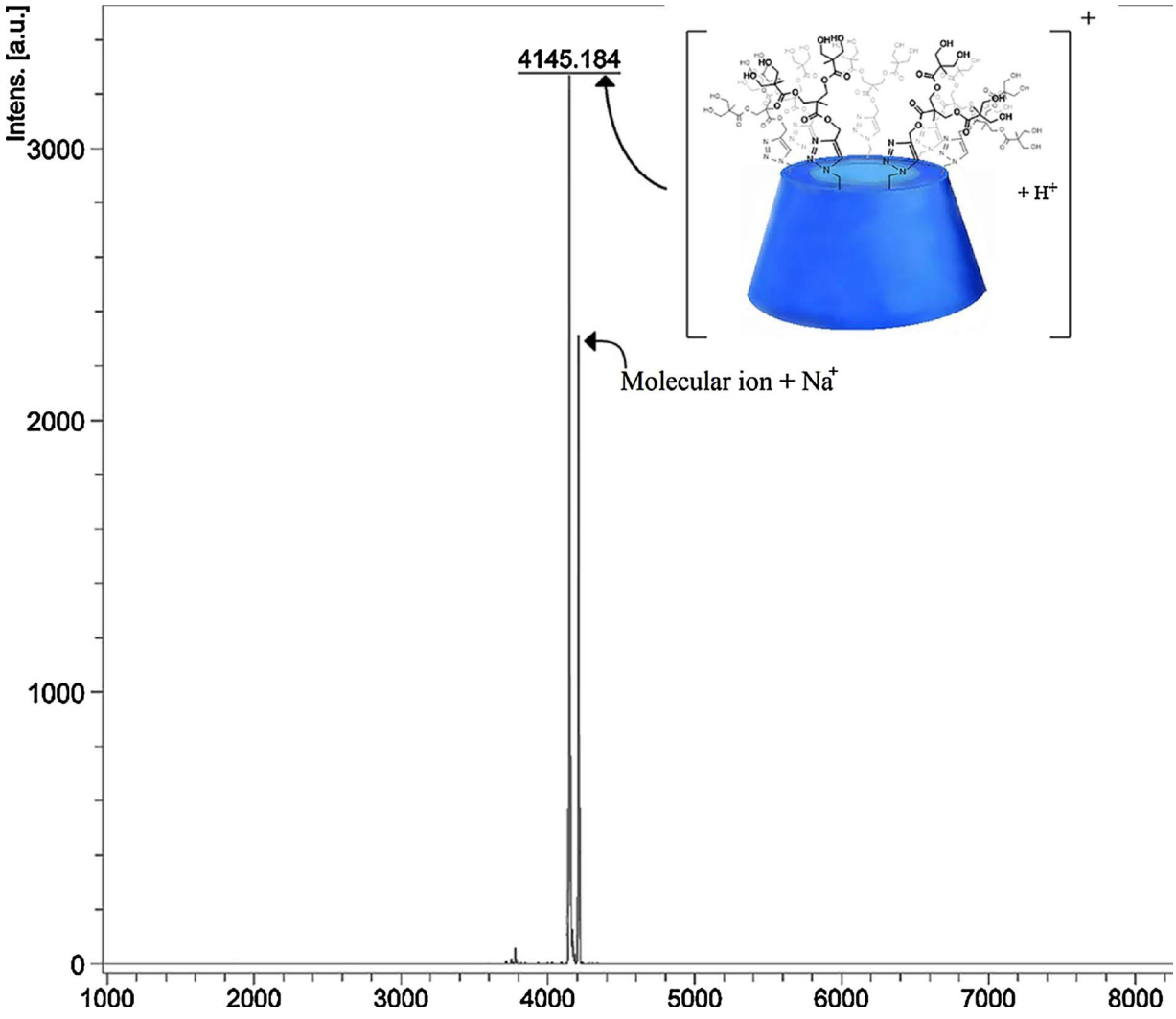

Fig. 1. MALDI-TOF MS of βCD[G2]-OH.

βCDs are those corresponding to the gauche-gauche (ω = −60°), gauche-trans (ω = 60°) and trans-gauche (ω = 180°) conformers (Cézard, Trivelli, Aubry, Djedaïni-Pilard, & Dupradeau, 2011). In our study, we identified a high percentage of gauche-gauche and gauche-trans conformations, demonstrating that some of the poly(ester) dendrons are exposed to water, while others are near the hydrophobic cavity (Fig. 3B and C). These theoretical conformations are supported by the NMR characterization.

3.4. Cell viability assays

Dendrimers are recognized as a major class of polymers within the nanomedicine field. However, their cytotoxic and hemolytic features are a hurdle to overcome. In this work, we constructed a dendritic material which is expected to keep the non-toxic profile of poly(ester) dendrons. To investigate the cytotoxicity of βCD[G2]-OH, experiments in HeLa cells were performed. The results (Fig. 4) indicate that βCD [G2]-OH did not altered the viability of the cells even at the highest concentration (10 mg/ml) evaluated (Table S2 Supplementary information). Although further biological experiments are needed, these promising results support our initial hypothesis and open the door to potentially exploit βCD[G2]-OH as a biomaterial.

3.5. Characterization of the βCD[G2]-OH/ABZ inclusion complex

To evaluate the ability of βCD[G2]-OH to form IC, the hydrophobic antiparasitic drug ABZ was chosen as a model molecule since its efficient complexation with βCD still remains a challenge (Chattah, Pfund, Zoppi, Longhi, & Garnero, 2017; Ferreira et al., 2015). Thus, the complex βCD[G2]-OH/ABZ and the PM were prepared and characterized by DSC and IR in the solid state. Additionally, an aqueous solution of the IC was characterized through UV–vis spectroscopy.

Fig. 5A displays the IC thermogram (**IV**) in which the endothermic peak at 210 °C, corresponding to the melting point of ABZ (**I**), disappears. In contrast, the thermogram of the PM (**III**), exhibits the transition temperatures of both, the melting point of ABZ and the loss of water molecules of βCD[G2]-OH (80–110 °C), confirming the complexation.

For the FT-IR analyses the bands of ABZ at 1631, 1599 and 1271 cm^{-1} (aromatic C=C, aromatic C=N and C−N stretching respectively) and those corresponding to βCD[G2]-OH at 3317, 2941, 1727 and 1200 cm^{-1} (O−H, aliphatic C−H, C=O and C−O−C stretching respectively) were followed (Fig. 5B). In the case of the PM (**III**), the bands corresponding to both components are clearly observed. On the other hand, the vibration pattern of βCD[G2]-OH was predominant in the IC (**IV**).

To investigate the ABZ complexation in an aqueous environment we employed UV–vis spectroscopy and changes in the maximum

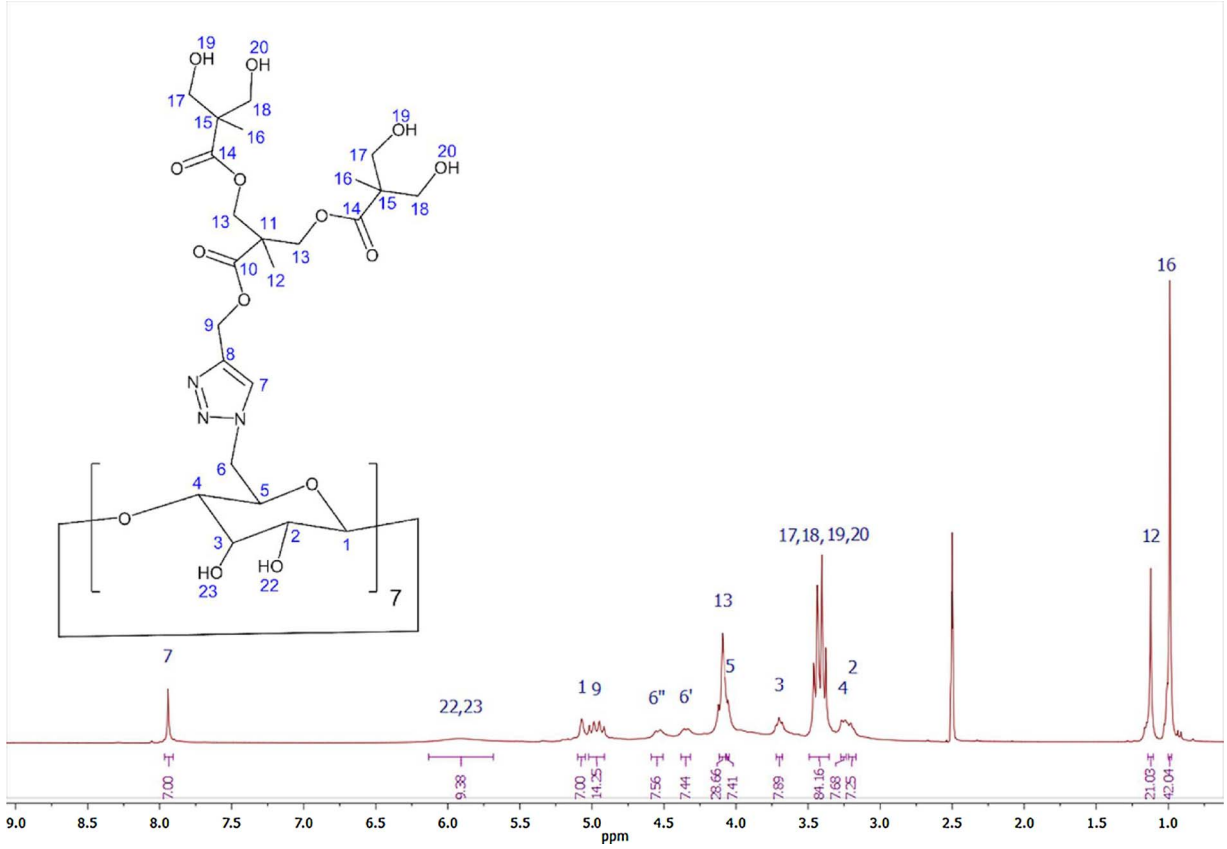

Fig. 2. ^{1}H NMR spectrum of βCD[G2]-OH in DMSO-d_6.

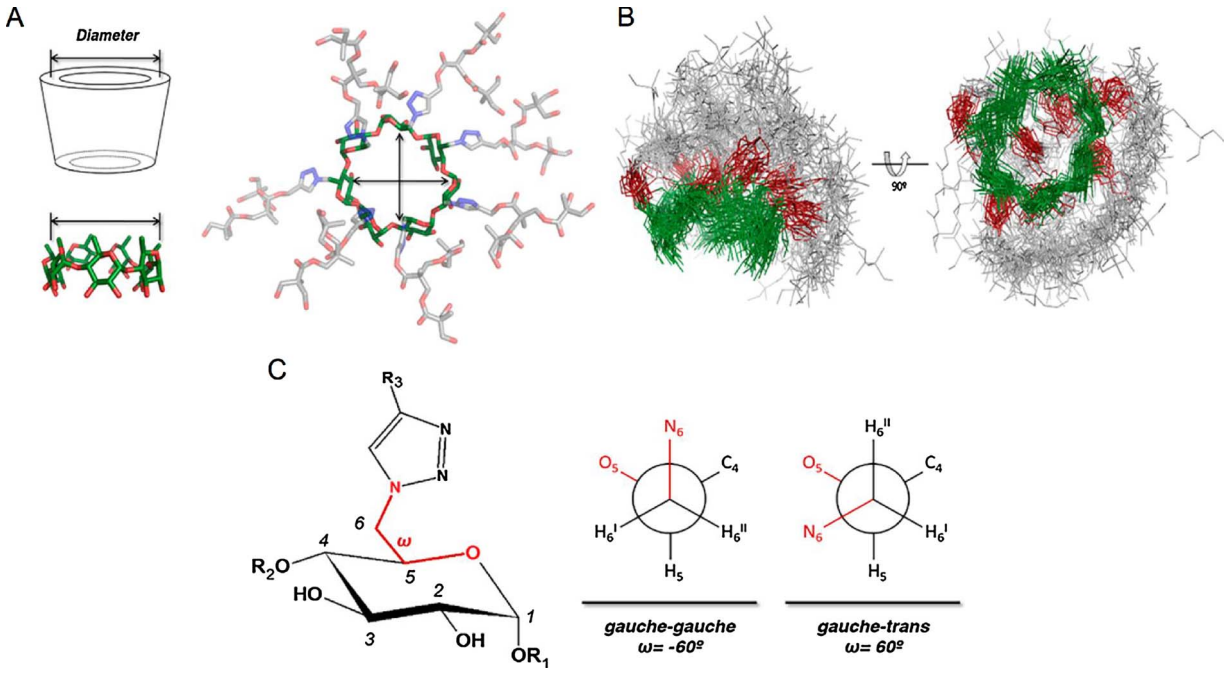

Fig. 3. Conformational analysis of βCD[G2]-OH. A) βCD diameter measurement in βCD[G2]-OH. B) Superimposition of more stable conformations. C) Dihedral angle ω, (omega, O5-C5-C6-N6) in βCD[G2]-OH, and the most common conformations.

absorption of ABZ were followed.

Fig. 6 shows that, when ABZ is complexed, its $n \rightarrow \pi^*$ maximum absorption at 298 nm is preserved. In contrast, the $\pi \rightarrow \pi^*$ absorption at 263 nm disappears, a phenomenon related to the entropy decrease of the guest. The slight blue shift of 4 nm (hypsochromic shift) indicates a higher electronic energy gap of the ABZ molecules that have been immobilized into the βCD[G2]-OH cavity. The mechanism of the blue shift can be also involving conformational changes entailing new intermolecular interactions (H-bonds, dipole-dipole interactions, among others) occurring in the interior of the cavity. Furthermore, this effect is

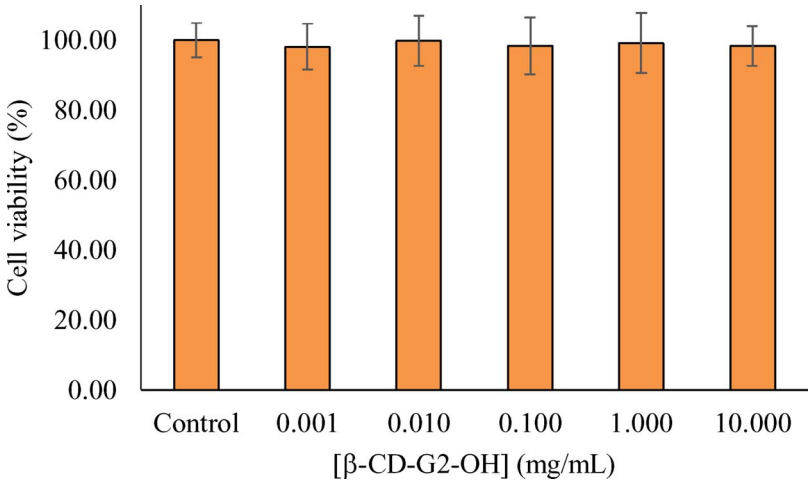

Fig. 4. Cell viability of βCD[G2]-OH in HeLa cells.

related to an excited state less polar than the ground state. These outcomes are in agreement with previous works characterizing CDs complexes by UV–vis (Jiang, Xu, Na, Jin, & Zhang, 2008; Hu, Zhang, Song, Gu, & Hu, 2012) and are an indicative that there is a host-guest interaction between ABZ and βCD[G2]-OH.

The βCD[G2]-OH/ABZ IC was successfully achieved through the simple cosolvency protocol established in this work. It must be highlighted that the IC was formed in a water/ethanol mixture, avoiding the use of organic solvents as DMSO, or other additives used in the attempt to obtain IC between ABZ and native βCD. It is worth noting that ethanol is allowed in pharmaceutical formulations, making our complex suitable for further biological applications.

3.6. Phase solubility diagram

According to the diagram obtained by the Higuchi and Connors' protocol (Fig. 7), βCD[G2]-OH/ABZ is classified as A_L type, assuming a 1:1 stoichiometry, with a K_c of 29636.17 M^{-1}, which represents the highest ABZ apparent aqueous solubility ever reported in the literature involving CDs (Pradines et al., 2014). The possible interactions between ABZ and the pristine dendrons (see Supplementary information for the [G2]-OH synthetic and structural details) were investigated. Fig. 7 shows that the UV–vis behavior of ABZ is not modified in the presence of the dendron moieties, indicating that the solubility of ABZ does not increase under these conditions. On the other hand, the increase of the ABZ solubility in the presence of βCD is negligible in comparison to our dendronized derivative.

The complexation efficiency (CE) has been proposed as an accurate parameter to determine the solubilizing effect of CDs on a specific guest. CE is the concentration ratio between CD in a complex and free CD and is calculated from the slope of the phase solubility diagram, and therefore, is independent of S_o and the intercept (Loftsson & Brewster, 2012). A CE = 0.133 was observed for the system βCD[G2]-OH/ABZ, that means that 2 out of every 15 βCD[G2]-OH molecules form a complex with ABZ. In contrast, the CE for βCD/ABZ was 0.007, indicating that 7 out of every 1000 βCD molecules are complexed with the guest. Such a great difference is reflected on the Solubility Enhancement Factor (F), which was 720 and 27.9 for βCD[G2]-OH and βCD respectively (Supplementary information) . These observations provide clear evidence of the remarkable complexation abilities of βCD [G2]-OH and a strong solubilization capacity for ABZ, which has been considered as a "difficult guest".

The CE and F parameters can be applied to other types of solubilizers (Loftsson & Brewster, 2012). For that reason, we also calculated them for the system [G2]-OH/ABZ. In this case, no changes were observed for the guest regarding CE, F nor UV spectroscopic behavior (Supplementary information), demonstrating the synergy arisen by the joining of βCD and [G2]-OH.

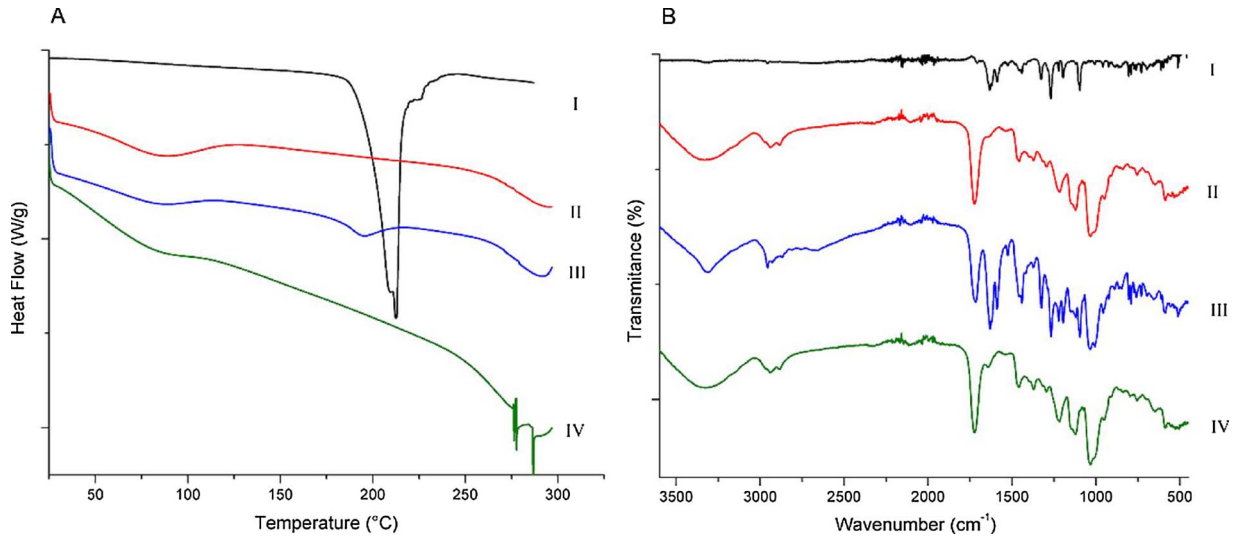

Fig. 5. A) DSC thermograms and B) FT-IR spectra of ABZ (**I**), βCD[G2]-OH (**II**), PM (**III**) and IC (**IV**).

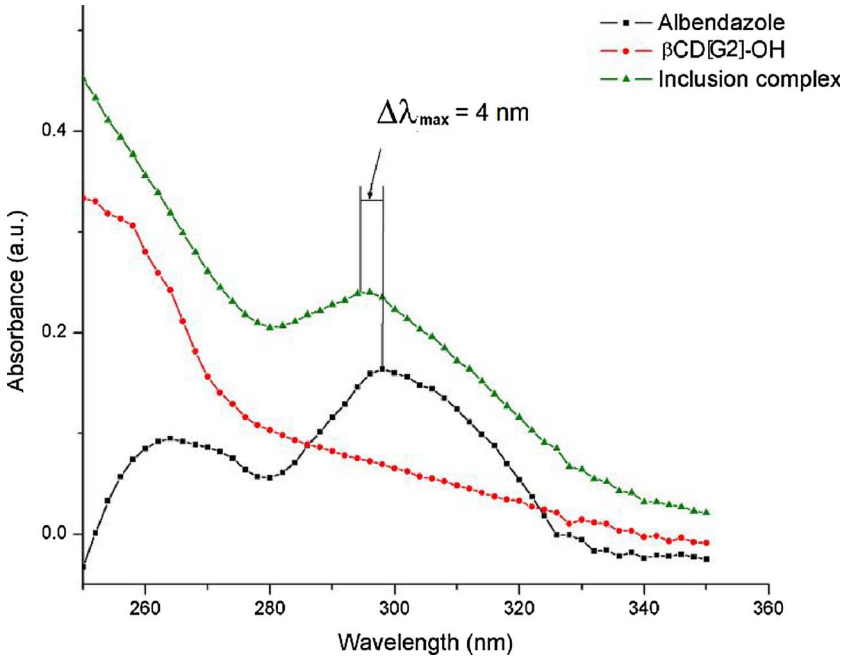

Fig. 6. UV–vis spectra of ABZ (1.88×10^{-2} mM, squares), βCD[G2]-OH (0.24 mM, circles) and IC (0.24 mM, triangles).

4. Conclusions

In this work, we presented a selective βCD derivatization with second generation poly(ester) dendrons in the seven positions of the βCD primary face. CuAAC click chemistry was the ideal approach to efficiently obtain the dendritic-shape derivative. The click reaction was followed by a simple work-up that allowed us to obtain the pure and monodisperse product in high yields. As we anticipated, the dendritic material showed a great aqueous solubility, which was even higher than that reported for SBE-βCD. At the same time, the computational studies revealed that the cavity remained available to form IC, a fact that was confirmed experimentally in our βCD[G2]-OH/ABZ system. Moreover, the complexation ability with ABZ was enhanced and the solubility of the guest was uniquely increased.

The dendritic material combined the physicochemical and biological features of both βCD and poly(ester) components, namely high aqueous solubility, no toxicity and enhanced complexation ability, confirming our hypothesis and demonstrating its potential use in pharmaceutical formulations, drug delivery and other fields.

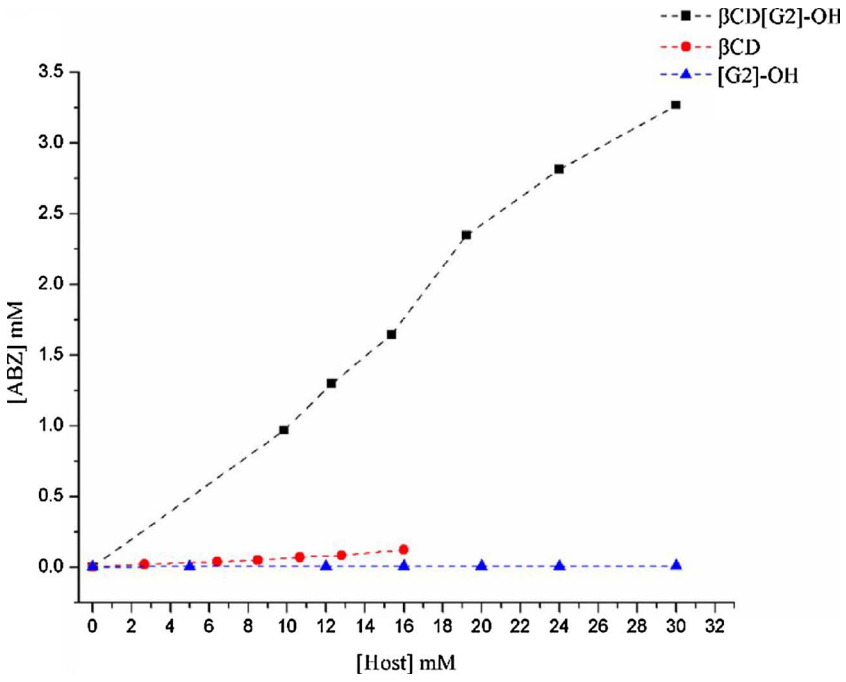

Fig. 7. Phase solubility diagram of βCD[G2]-OH/ABZ, βCD/ABZ and [G2]-OH/ABZ.

Acknowledgments

Authors acknowledge the financial support to Consejo Nacional de Ciencia y Tecnologia-Mexico (CONACyT) (project 239672) and Programa de Apoyo a Proyectos de Investigación e Innovación Tecnológica (PAPIIT-UNAM) (IN101109-3). Also thanks to M. Sc. Lucero Rios Ruiz and Q. Eréndira García Ríos for MALDI-MS spectra, Q.F.B. Karla Eriseth Reyes Morales for DSC thermograms, M. Sc. Elizabeth Huerta Salazar and Q. Ma. De los Angeles Peña Gonzales for NMR spectra. LD acknowledge DGTIC-UNAM for the support received

in the use of the HP Cluster Platform 3000SL supercomputer (Miztli), project LANCAD-UNAM-DGTIC-306. YRA thanks to Programa de Apoyo a la Investigación y el Posgrado (PAIP 5000-9157), Facultad de Química, UNAM and to Edward H. Trager (University of Michigan) for providing language revision.

Appendix A. Supplementary data

Supplementary material related to this article can be found, in the online version, at doi:https://doi.org/10.1016/j.carbpol.2017.12.049

References

Abraham, M. J., Murtola, T., Schulz, R., Páll, S., Smith, J. C., Hess, B., & Lindah, E. (2015). Gromacs: High performance molecular simulations through multi-level parallelism from laptops to supercomputers. *SoftwareX, 1–2*, 19–25. http://dx.doi.org/10.1016/j.softx.2015.06.001.

Antoniuk, I., & Amiel, C. (2016). Cyclodextrin-mediated hierarchical self-assembly and its potential in drug delivery applications. *Journal of Pharmaceutical Sciences, 105*(9), 2570–2588. http://dx.doi.org/10.1016/j.xphs.2016.05.010.

Ashton, P. R., Königer, R., Stoddart, J. F., Alker, D., & Harding, V. D. (1996). Amino acid derivatives of β-cyclodextrin. *The Journal of Organic Chemistry, 61*(3), 903–908. http://dx.doi.org/10.1021/jo951396d.

Captisol. (2017). http://www.captisol.com/. Retrieved July 20, 2017, from http://www.captisol.com/.

Carlmark, A., Malmström, E., & Malkoch, M. (2013). Dendritic architectures based on bis-MPA: Functional polymeric scaffolds for application-driven research. *Chemical Society Reviews, 42*(13), 5858–5879. http://dx.doi.org/10.1039/c3cs60101c.

Cézard, C., Trivelli, X., Aubry, F., Djedaïni-Pilard, F., & Dupradeau, F.-Y. (2011). Molecular dynamics studies of native and substituted cyclodextrins in different media: 1. Charge derivation and force field performances. *Physical Chemistry Chemical Physics: PCCP, 13*(33), 15103–15121. http://dx.doi.org/10.1039/c1cp20854c.

Challa, R., Ahuja, A., Ali, J., & Khar, R. K. (2005). Cyclodextrins in drug delivery: An updated review. *AAPS PharmSciTech, 6*(2), E329–E357. http://dx.doi.org/10.1208/pt060243.

Chattah, A. K., Pfund, L. Y., Zoppi, A., Longhi, M. R., & Garnero, C. (2017). Toward novel antiparasitic formulations: Complexes of albendazole desmotropes and β-cyclodextrin. *Carbohydrate Polymers, 164*, 379–385. http://dx.doi.org/10.1016/j.carbpol.2017.01.098.

Crini, G. (2014). Review: A history of cyclodextrins. *Chemical Reviews, 114*(21), 10940–10975. http://dx.doi.org/10.1021/cr500081p.

DeLano, W. L. (2002). *The PyMOL molecular graphics system, version 0.99.* Schrödinger LLChttp://doi.org/citeulike-article-id:240061.

Faugeras, P.-A., Boëns, B., Elchinger, P.-H., Brouillette, F., Montplaisir, D., Zerrouki, R., ... Lucas, R. (2012). When cyclodextrins meet click chemistry. *European Journal of Organic Chemistry, 2012*(22), 4087–4105. http://dx.doi.org/10.1002/ejoc.201200013.

Ferreira, M. J. G., García, A., Leonardi, D., Salomon, C. J., Lamas, M. C., & Nunes, T. G. (2015). (13)C and (15)N solid-state NMR studies on albendazole and cyclodextrin albendazole complexes. *Carbohydrate Polymers, 123*, 130–135. http://dx.doi.org/10.1016/j.carbpol.2015.01.031.

Forester, T. R., & Smith, W. (1998). SHAKE, rattle, and roll: Efficient constraint algorithms for linked rigid bodies. *Journal of Computational Chemistry, 19*(1), 102–111. http://dx.doi.org/10.1002/(SICI)1096-987X(19980115)19:1<102::AID-JCC9>3.0.CO;2-T.

García, A., Leonardi, D., & Lamas, M. C. (2016). Promising applications in drug delivery systems of a novel β-cyclodextrin derivative obtained by green synthesis. *Bioorganic & Medicinal Chemistry Letters, 26*(2), 602–608. http://dx.doi.org/10.1016/j.bmcl.2015.11.067.

Higuchi, T., & Connors, K. A. (1965). Phase solubility techniques. *Advanced Analytical Chemistry of Instrumentation, 4*, 117–210.

Hu, L., Zhang, H., Song, W., Gu, D., & Hu, Q. (2012). Investigation of inclusion complex of cilnidipine with hydroxypropyl-β-cyclodextrin. *Carbohydrate Polymers, 90*(4), 1719–1724. http://dx.doi.org/10.1016/j.carbpol.2012.07.057.

Ihre, H., Hult, A., Fréchet, J. M. J., & Gitsov, I. (1998). Double-stage convergent approach for the synthesis of functionalized dendritic aliphatic polyesters based on 2,2-bis (hydroxymethyl)propionic acid. *Macromolecules, 31*(13), 4061–4068. http://dx.doi.org/10.1021/ma9718762.

Ihre, H. R., Padilla De Jesús, O. L., Szoka Francis, C., & Fréchet, J. M. J. (2002). Polyester dendritic systems for drug delivery applications: Design, synthesis, and characterization. *Bioconjugate Chemistry, 13*(3), 443–452. http://dx.doi.org/10.1021/bc010102u.

Jiang, H., Xu, Y., Na, L., Jin, R., & Zhang, S. (2008). UV–vis spectral analysis of inclusion complexes between β-cyclodextrin and aromatic/aliphatic guest molecules. *Current Drug Discovery Technologies, 5*(2), 173–176. http://dx.doi.org/10.2174/157016308784746283.

Jorgensen, W. L., Chandrasekhar, J., Madura, J. D., Impey, R. W., & Klein, M. L. (1983). Comparison of simple potential functions for simulating liquid water. *The Journal of Chemical Physics, 79*(2), 926. http://dx.doi.org/10.1063/1.445869.

Juanola-Feliu, E., Colomer-Farrarons, J., Miribel-Catal, P., Samitier, J., & Valls-Pasola, J. (2012). Market challenges facing academic research in commercializing nano-enabled implantable devices for in-vivo biomedical analysis. *Technovation, 32*(3–4), 193–204. http://dx.doi.org/10.1016/j.technovation.2011.09.007.

Kolb, H. C., Finn, M. G., & Sharpless, K. B. (2001). Click chemistry: Diverse chemical function from a few good reactions. *Angewandte Chemie International Edition, 40*(11), 2004–2021. http://dx.doi.org/10.1002/1521-3773(20010601)40:11<2004::AID-ANIE2004>3.0.CO;2-5.

Kumari, R., Kumar, R., & Lynn, A. (2014). G-mmpbsa—A GROMACS tool for high-throughput MM-PBSA calculations. *Journal of Chemical Information and Modeling, 54*(7), 1951–1962. http://dx.doi.org/10.1021/ci500020m.

Lindorff-Larsen, K., Piana, S., Palmo, K., Maragakis, P., Klepeis, J. L., Dror, R. O., ... Shaw, D. E. (2010). Improved side-chain torsion potentials for the Amber ff99SB protein force field. *Proteins: Structure, Function and Bioinformatics, 78*(8), 1950–1958. http://dx.doi.org/10.1002/prot.22711.

Loftsson, T., & Brewster, M. E. (2012). Cyclodextrins as functional excipients: Methods to enhance complexation efficiency. *Journal of Pharmaceutical Sciences, 101*(9), 3019–3032. http://dx.doi.org/10.1002/jps.23077.

Frisch, M. J., Trucks, G., Schlegel, W., Schlegel, H. B., Scuseria, G. E., Robb, M. A., Cheeseman, J. R., Scalmani, G., Barone, V., Mennucci, B., Petersson, G. A., Nakatsuji, H., Caricato, M., Li, X., Hratchian, H. P., Izmaylov, A. F., Bloino, J., Zheng, G., Sonnenberg, J. L., Hada, M., Ehara, M., Toyota, K., Fukuda, R., Hasegawa, J., Ishida, M., Nakajima, T., Honda, Y., Kitao, O., Nakai, H., Vreven, T., Montgomery, J. A., Jr., Peralta, J. E., Ogliaro, F., Bearpark, M., Heyd, J. J., Brothers, E., Kudin, K. N., Staroverov, V. N., Kobayashi, R., Normand, J., Raghavachari, K., Rendell, A., Burant, J. C., Iyengar, S. S., Tomasi, J., Cossi, M., Rega, N., Millam, J. M., Klene, M., Knox, J. E., Cross, J. B., Bakken, V., Adamo, C., Jaramillo, J., Gomperts, R., Stratmann, R. E., Yazyev, O., Austin, A. J., Cammi, R., Pomelli, C., Ochterski, J. W., Martin, R. L., Morokuma, K., Zakrzewski, V. G., Voth, G. A., Salvador, P., Dannenberg, J. J., Dapprich, S., Daniels, A. D., Farkas, Ö., Foresman, J. B., Ortiz, J. V., & Cioslowski, J. (2009). *Gaussian 09, revision E.01.* Wallingford, CT: Gaussian, Inc.

Ma, D.-Y., Zhang, Y.-M., & Xu, J.-N. (2016). The synthesis and process optimization of sulfobutyl ether β-cyclodextrin derivatives. *Tetrahedron, 72*(22), 3105–3112. http://dx.doi.org/10.1016/j.tet.2016.04.039.

Pradines, B., Gallard, J.-F., Iorga, B. I., Gueutin, C., Loiseau, P. M., Ponchel, G., ... Bouchemal, K. (2014). Investigation of the complexation of albendazole with cyclodextrins for the design of new antiparasitic formulations. *Carbohydrate Research, 398*, 50–55. http://dx.doi.org/10.1016/j.carres.2014.06.008.

Promega. (2012). CellTiter 96 Non-Radioactive Cell Proliferation Assay Quick Protocol, FB045.

Schmidt, B. V. K. J., Hetzer, M., Ritter, H., & Barner-Kowollik, C. (2014). Complex macromolecular architecture design via cyclodextrin host/guest complexes. *Progress in Polymer Science, 39*(1), 235–249. http://dx.doi.org/10.1016/j.progpolymsci.2013.09.006.

Schneider, H.-J., Hacket, F., Rüdiger, V., & Ikeda, H. (1998). NMR studies of cyclodextrins and cyclodextrin complexes. *Chemical Reviews, 98*(5), 1755–1786. http://dx.doi.org/10.1021/cr970019t.

Stepniak, P., Lainer, B., Chmurski, K., & Jurczak, J. (2017). The effect of urea moiety in amino acid binding by β-cyclodextrin derivatives: A 1000-fold increase in efficacy comparing to native β-cyclodextrin. *Carbohydrate Polymers, 164*, 233–241. http://dx.doi.org/10.1016/j.carbpol.2017.02.018.

Svenson, S. (2015). The dendrimer paradox-high medical expectations but poor clinical translation. *Chemical Society Reviews, 44*(12), 4131–4144. http://dx.doi.org/10.1039/C5CS00288E.

Varan, G., Varan, C., Erdoğar, N., Hincal, A. A., & Bilensoy, E. (2017). Amphiphilic cyclodextrin nanoparticles. *International Journal of Pharmaceutics*. http://dx.doi.org/10.1016/j.ijpharm.2017.06.010.

Zhao, W., & Zhong, Q. (2012). Recent advance of cyclodextrins as nanoreactors in various organic reactions: A brief overview. *Journal of Inclusion Phenomena and Macrocyclic Chemistry, 72*(1), 1–14. http://dx.doi.org/10.1007/s10847-011-9983-9.